Application of experimental methodology design to optimize adsorption parameters for Sulfametaxazole and Trimethoprim removal using natural clay

YOUSRA AISSAOUI [1], MALIKA TRABELSI-AYADI [2], IBTISSEM GHORBEL-ABID [1,2]
[1]Useful Materials Laboratory (LMU),
National Institute for Physical and Chemical Research and Analysis (INRAP),
BiotechPole Ariana 2020,
TUNISIA

[2]Laboratory of Application Chemistry to the Resources and Natural Substances and the Environment (LACReSNE),
Faculty of Science of Bizerte, University of Carthage,
Zarzouna, Bizerte 7021,
TUNISIA

Correspondence Author

Abstract: - Conventional water treatment plants are often not equipped to effectively eliminate micropollutants such as antibiotics. Sulfamethoxazole (SMX) and trimethoprim (TMP) are widely used in human and veterinary treatment. This study aims to remove these two antibiotics from aqueous solution using natural clay as an adsorbent. A Box-Behnken matrix was used to model and optimize the process. the textural, structural, and morphological properties of raw and purified natural clay were studied. Four independent variables were selected: the initial concentration, pH, contact time, and temperature. Under the experimental conditions, the system reached equilibrium in 80 min. The maximum adsorption of SMX and TMP was approximately 98%. The maximum adsorption capacity was estimated to be 250 $mg.g^{-1}$ and 190 $mg.g^{-1}$ at pH 6. According to the Box-Behnken model, high correlation coefficient values and p values greater than 0.05 corresponded to a good fit to the optimal combination of process parameters.

Key-Words: - Adsorption, Optimization, Sulfamethoxazole, Trimethoprim, Natural clay, green adsorbents, Box-Behnken design, Response surface methodology, sustainable development.

Received: June 23, 2025. Revised: September 25, 2025. Accepted: October 27, 2025. Published: May 5, 2026.

1 Introduction

Chemical and pharmaceutical pollution represent a negative impact on the environment and a serious threat to global water quality, [1], [2], causing a significant deterioration in aquatic ecosystems and endangering human health, [3]. These contaminants of emerging concern (CECs) are released into the environment directly by pharmaceutical factories' discharges or by chemical reactions like human excrement, household waste, and hospital waste, [4]. Globally, over 600 pharmaceutical compounds have been detected in surface, ground, and drinking water at concentrations ranging from $ng.L^{-1}$ to $\mu g.L^{-1}$, [5], [6]. Focusing on the antibiotics are used in aquaculture sector to prevent and treat bacterial infections to ensure the healthy and productivity of farmed aquatic species, Sulfamethoxazole (SMX) and trimethoprim (TMP), commonly operated together as co-trimoxazole (e.g., Bactrim®), are bacteriostatic agents effective against a range of bacterial infections, including urinary tract infections, respiratory illnesses, and gastrointestinal disorders, [7]. Hence, an extensive portion of these antibiotics is not metabolized by the organisms and released directly into surrounding waters by excretion or uneaten medicated feed, leading to antibiotic residues in aquatic ecosystems, [8]. However, the 2030 UN Agenda of Sustainable Development Goals (SDGs) has highlighted the importance of clean water, sustainable food production, and responsible consumption, emphasizing their mutuality within the model of a circular economy, which aims to supply people with food and save the planet from alteration, [9]. In this context, cost-effective removal of antibiotics from aqueous effluents is crucial to maintaining ecological balance, supporting safe food systems, and promoting resource efficiency, [10], [11]. Conventional wastewater treatment processes, such as activated sludge systems, achieve only moderate removal efficiencies (48–77%) for this sulfonamide and diaminopyrimidine antibiotics, resulting in their persistence in treated effluents, surface waters, and even drinking water sources at concentrations ranging from ng.L^{-1} to µg.L^{-1}, [12], [13]. This persistence exacerbates the development of antibiotic resistance genes (ARGs), potentially fostering superbugs and disrupting microbial communities in receiving waters. In terms of removal methods for sulfamethoxazole and trimethoprim from aquaculture effluents, several approaches are used, such as physical and chemical treatments, including adsorption, reverse osmosis, constructed wetlands, electrooxidation, and advanced oxidation processes like ozonation, [14]. Woodchip bioreactors have shown an effective removal if SMX and TMP when the microbial degradation is promoting with specific conditions provides substantial reductions in antibiotic discharge risk into the environment with a removal retention have attended (~77-89%) for TMP and (~63-77%) for the SMX, this innovative tool for aquaculture effluent management can be considered like green approach, [15], but their effectiveness is depending always by the heavily on microbial community health and the environmental conditions such as temperature, dissolved oxygen, environment's pH and the hydraulic retention time. Since not all antibiotics are equally well removed, for example, florfenicol shows poor adsorption. Moreover, the process is relatively slow compared to some advanced oxidation methods, limiting rapid treatment needs. In contrast, the adsorption method offers distinct advantages for antibiotic removal in aquaculture environments. The use of activated carbon, biochar, and natural clay materials as adsorption techniques is still one of the most reliable and widely used methods for removing antibiotics from aquaculture and municipal effluents. Considering the high adsorption capacity, the natural clays such as montmorillonite exhibit high adsorption capacities for antibiotics like tetracycline (more than 227mg.L^{-1}) and likely for sulfamethoxazole and trimethoprim due to similar adsorption mechanisms like electrostatic interactions and chemical bonding, [16]. Also, the natural clays are abundant, inexpensive, and require minimal processing, making them highly economical for large-scale applications, [17], [18]. In fact, modified and unmodified clays possess favorable surface area, porosity, and chemical properties that enhance adsorption, providing stable, reusable adsorbents with little degradation. Overall, natural clays are environmentally benign and do not introduce harmful byproducts during adsorption, making them sustainable options for aquaculture effluent treatment, [19], [20]. Adsorption methods are considered the best technique for removing antibiotics due to their high efficiency, design simplicity, low cost, and minimal sludge. Response surface methodology (RSM) has become widely employed in the last few decades to examine the interaction between the variable's ant their effect to responses variables in chemical processes. Experimental design methods could not only maximize the antibiotic removal but also could reduce treatment time and solvent use, adopting a sustainable and cost-effective green strategy for wastewater effluent management. Antibiotic removal study used Box-Behnken design (BBD) and response surface methodology (RSM) as an efficient exploration of the effects of key process variables such as contact time, adsorbent dosage, biomass, and antibiotic concentration. Despite the central composite designs (CCD), the BBD does not include experiments at the extreme vertices of the design space; this characteristic is an advantage due to the ability to operate under extreme conditions, which can lead to the adsorbent degradation and be impractical. Consequently, BBD is considered a safer and more approach for experimental optimization in environmental and chemical applications. Consequently, BBD is considered a safer and more stable approach for experimental optimization in environmental and chemical handling applications, [21]. Overall, the Box–Behnken Design offers an optimal balance between experimental economy, statistical robustness, and predictive capability, making it a powerful tool for optimizing adsorption processes and modeling pollutant removal mechanisms. It has been reported that o the removal of tetracycline and chloramphenicol by aquatic plants using the BBD model has been evaluated by the optimal interaction effect between the contact time, plant biomass, and initial antibiotic concentration, to attend to 84% removal, [22]. Box-Behnken Design was applied to optimize oxytetracycline removal, well showing the ability of the model to study the complex interactions between the pH, Temperature, and different antibiotic concentrations, with more and best condition to identify the effective removal condition by reducing the number of experiments and solvent/ adsorbent application, [23], [24].

This study focuses on the characterization of local natural clay as an adsorbent. The raw and purified clay has been characterized by different methods for well-determinate their properties well. Furthermore, the adsorption isotherm models were applied to assess the adsorption mechanism, accomplished by the thermodynamics studies to improve the adsorption process. In addition, the parameters on the efficiency of Sulfametaxazole and trimethoprim removal from aqueous solution using a smectite adsorbent were evaluated by the BBD-RSM approach.

2 Materials and methods

2.1 Reagents and materials

Trimethoprim and Sulfamethoxazole were purchased from Sigma Aldrich. The physicochemical properties and the chemical structures of both compounds are shown in Table 1 (Appendix). Individual stock standard solutions at a concentration of 10 $mg.L^{-1}$, were prepared in methanol and stored at -18 $^{\circ C}$ in dark glass vials. The standards solutions were prepared daily by appropriate dilution of the stock solution with water. Methanol and Acetonitrile (ACN) were of HPLC grade. These solvents were obtained from VWR (BDH chemicals). Sodium phosphate monobasic monohydrate (Purity N99.0%) and sodium phosphate (Purity N99.0%) were from VWR.

2.2 Sampling and preparation of the studied clay samples

Tunisian natural clays have interesting potential for the elimination of pollutants. Their use for wastewater treatment is promising. The two natural clays used in this study are of Tunisian origin, Ain Mestir clay (noted AM). The nature of the AM clay is not known previously; its purification was the subject of the first step of the study. Its two raw and purified fractions were characterized by the usual techniques. The region of Aïn Mestir, located in the governorate of Bizerte, northern Tunisia (37°12'19"N, 10°11'23"E). This area presents interesting geographical and pedological characteristics, particularly in terms of relief, soil, and hydrology. This region, with a varied topography, includes moderate hills and valleys conducive to water retention, which promotes the development of local vegetation. Like the entire region of Bizerte, Aïn Mestir is fed by shallow groundwater tables, in interaction with seasonal rivers, which undergo variations according to annual precipitation. In order to determine the chemical compositions of adsorbents as well as their physico-chemical properties, the purification step of raw clays is very important to isolate the fine fractions, and to obtain a swellable clay, of good dispersion in water and high cation exchange capacity. The procedure for purifying raw clays generally allows the decomposition of carbonates, the dissolution of hydroxides and metal oxides (Fe, Al), the elimination of amorphous silica, as well as the oxidation of existing organic matter. After the removal of impurities by sieving large particles and coarse impurities, the sample was removed using a 100-micrometer sieve. This allowed the removal of unwanted debris and particles.

2.3 Sorption studies

Batch system experiments were performed to carry out the adsorption mechanism on the two clays. In each experiment, the solution containing 45 mL of antibiotic with a concentration of 100 mg. L-1 was used. The solution's pH was adjusted to 6 using 0.1 M HCl and 0.1 M NaOH. A quantity of 0.1 g of the adsorbent was added to the solution and subjected to an ultrasonic bath for 180 min. With the adsorbent in glass vessels, using a Stuart rotator (SB3) at a constant stirring speed (250 rpm) and a controlled temperature (T =25°C and 80°C). When the adsorption equilibrium was reached, the sample was separated from the aqueous solution using a filtration method with a 0.45µm Whatman cellulose nitrate membrane. Afterwards, the analysis of the residual solution was performed by UV-visible absorption spectrophotometry at λmax = 270 nm (UV Visible spectrophotometer Secomam).

The percentage removal of the drug and the amount of antibiotic adsorbed on clay (q) were calculated by Eq. (1) and (2), respectively:

$$q = \frac{C_0 - Ce}{m} \times V \qquad \textbf{(1)}$$

Where q: Quantity of drug adsorbed per gram of adsorbent (mg.g-1); C0: Initial concentration (mg.1-1); Ce: Equilibrium concentration (mg/l); m (g.L-1) is the adsorbent dose used in the adsorption experiments, and V (L): the total volume of the solution.

$$R(\%) = \frac{C_0 - Ce}{C0} \times 100 \qquad \textbf{(2)}$$

2.4 Experimental design

To determine the optimal conditions for the adsorption of the two antibiotics on two types of clay, we selected the following independent variables for this study are: the concentration of each molecule (10 mg. L-1 to 100 mg. L-1), pH (4-9), contact time (10min-150 min) and the temperature (40°, 80°). The four independent factors studied are: initial antibiotic concentration, pH, temperature, and contact time. Their areas of variation are presented in the following table (Table 1):

Table 1: Values of the independent variables
Source: created by authors.

	Factor	Unit	Centre	variation Path
X1	Temperature	°C	60	20
X2	Concentration	Mg. L^{-1}	55	45
X3	pH		6,54	2,5
X4	Contact time	min	110,0	90,0

The studied plan is based on 27 experiments presented in Table 2. The matrix of experiments given in Table 2 gathers the tests given in order and the values of adsorption rates obtained for each test. The experimental data were fitted to a second-order model (Eq. (3)):

Y1=b0+b1X1+b2X2+b3X3+b4X4+b11X12+b22 X22+b33X32+b44X42+b12X1X2+b13X1X3+b14X 1X4+b23X2X3+b24X2X4+b34X3X4

With: Y is the measured response, b0 is the model constant, bi are linear coefficients, and X1, X2, X3, and X4 are coded variables. To generate the matrix design, statistical analysis, and regression models, the software used is NEMROD-W version 9901. The significance of the second-order models was evaluated by analysis of variance (ANOVA).

Table 2: BBD matrix for removal of SMX and TMP.
Source: created by authors.

Exp number	X1	X2	X3	X4
1	-1.000	-1.0000	0.0000	0.0000
2	1.000	-1.000	0.0000	0.0000
3	-1.000	1.000	0.0000	0.0000
4	1.000	1.000	0.0000	0.0000
5	-1.000	0.0000	-1.000	0.0000
6	1.000	0.0000	-1.000	0.0000
7	-1.000	0.0000	1.000	0.0000
8	1.000	0.0000	1.000	0.0000
9	-1.000	0.0000	0.0000	-1.000
10	1.000	0.0000	0.0000	-1.000
11	-1.000	0.0000	0.0000	1.000
12	1.000	0.0000	0.0000	1.000
13	0.0000	-1.000	-1.000	0.0000
14	0.0000	1.000	-1.000	0.0000
15	0.0000	-1.000	1.000	0.0000
16	0.0000	1.000	1.000	0.0000
17	0.0000	-1.000	-1.000	-1.000
18	0.0000	1.000	0.0000	-1.000
19	0.0000	-1.000	0.0000	1.000
20	0.0000	1.000	0.0000	1.000
21	0.0000	0.0000	-1.000	-1.000
22	0.0000	0.0000	1.000	-1.000
23	0.0000	0.0000	-1.000	1.000
24	0.0000	0.0000	1.000	1.000
25	0.0000	0.0000	0.0000	0.0000
26	0.0000	0.0000	0.0000	0.0000
27	0.0000	0.0000	0.0000	0.0000

Figure 1 (Appendix) shows that no other interaction among X1, X2, X3 (pH), and X4 (contact time) has been significant for either AMb or AMp. This means that the combinations involving pH and time of contact do not significantly influence adsorption for both types of clay in this configuration. These graphs present the results of the tests of normality, showing that the residuals of the two models are in accordance with the assumption of normality, which is preferred for the justification and validity of the models. It is noted that the Q-Q Plot for TMP: The points continue approximately along the red diagonal line, which indicates that the residues follow a reasonable normal distribution, with some slight deviations at the ends. The same, for Q-Q Plot for SMX: the points are close to the line, which also confirms that the residues for SMX follow a normal distribution.

3 Results and discussion

3.1 Characterization of the adsorbent

The geological source and the formation process are mainly responsible for the chemical composition. Typically, the major elements are composed of hydrated aluminum silicates and other minor elements, such as iron or alkali and alkaline-earth metals, [25]. The clay used in this study was collected from a natural deposit in Tunisia and subsequently purified to obtain two materials adsorbents: the raw clay (AMb) and the purified clay (AMp). These materials were characterized using complementary techniques such as Energy Dispersive X-ray Spectroscopy (EDS), X-ray Diffraction (XRD), and Scanning Electron Microscopy (SEM), to determine their chemical composition, mineralogical structure, and physicochemical properties have used in adsorption experiments for Sulfamethoxazole (SMX) and Trimethoprim (TMP).

3.1.1 Chemical composition

Table 2 (Appendix) shows the chemical elements of raw and purified clay, which show that there are differences between the two types of samples, with lower levels of impurities in the purified clays. EDS analysis revealed notable differences between the raw and purified clay samples. The raw clay (AMb) contained high levels of oxygen (45.09 wt%), carbon (23.62 wt%), silicon (11.36 wt%), and aluminium (6.04 wt%), alongside smaller amounts of calcium (9.02 wt%), fluorine (3.07 wt%), potassium (1.15 wt%), and magnesium (0.65 wt%). This composition indicates that the natural material is an aluminosilicate rich in clay minerals (primarily smectite, with minor kaolinite or illite), while also containing non-clay impurities such as carbonates ($CaCO_3$) and organic matter. After purification, the purified clay (AMp) showed enrichment in the main clay-forming elements: oxygen (54.90 wt%), silicon (17.67 wt%), and aluminum (9.30 wt%) were dominant, with minor elements such as calcium (13.79 wt%), magnesium (1.01 wt%), potassium (1.76 wt%), and fluorine (1.58 wt%) present in trace amounts.

The EDS analysis of natural clays confirms the presence of elements usually contained in aluminosilicate materials (SiO_2 and Al_2O_3) (Figure 2 (Appendix)). Additionally, the absence of detectable carbon confirms that organic matter and carbonates were effectively removed. The high Si/Al ratio indicates a predominance of silica-rich smectite layers, contributing to a larger surface area and strong adsorption potential. In this case, the SEM technique has been used to study the morphological properties of the natural clays. The analyzed samples showed a gross fraction and a compacted structure, where a porous structure can be evidenced, which provided porosity to the clay materials. Also, SEM micrographs provide insight into the texture and morphology of the clay, revealing mineralogical agglomerates. Images at different magnifications (Figure 3 (Appendix)) show that calcite appears as well-defined aggregates, while quartz is present as small grains. These observations confirm the heterogeneous nature of the raw clay and illustrate the microstructural features that influence adsorption capacity.

3.1.2 Mineralogical Structure

As can be seen in Figure 4 (Appendix), XRD analysis typically shows that both AMb and AMp clays are dominated by smectite-type layers, with traces of montmorillonite and kaolinite, the typical assigned to bentonite, consisted of montmorillonite (d spacing (M) = ~12.00 Å, 4.65 Å, 2.56 Å), Kaolinite (d spacing (K) = ~7.141 Å, 3.56 Å) a significant proportion of Calcite (d spacing (Ca) = ~3.07 Å). The purification strongly reduces the intensity of quartz and calcite peaks, which is explained by the partial removal of the crystalline impurities. The purification improves the clay's textural properties. The removal of carbonates, iron oxides, and organic matter increases the specific surface area, pore volume, and cation exchange capacity (CEC), all essential for efficient adsorption, [25], [26]. The use of Tunisian clays for the adsorption of antibiotics highlights their potential in the treatment of contaminated water. The clay can capture a significant amount of these pollutants through specific interactions such as the electrostatic interactions, hydrogen bonding, and cation exchange mechanisms, [17], [18]. Additionally, the fundamental structural features of clays, including the Si–Al–O arrangement, layered features, and isomorphous substitutions in tetrahedral sheets, provide additional active sites for adsorption and contribute to the cation-exchange capacity to improve their performance as adsorbents, [27], [28], [29].

3.2 Response surface methodology (RSM) results

In the field of experimental design, the Box-Behnken plan is a very useful statistical approach for studying interactions between several factors and optimizing processes. This type of experimental design considerably reduces the number of tests required compared to a complete factorial design, while retaining the possibility of modeling non-linear responses. In this study, the Box-Behnken model demonstrated an excellent fit of the experimental data, with coefficients of determination that are higher, R2= 0.99, and the adjusted R2 = 0.99, this is providing the strong concordance between the predicted and observed values. A coefficient of determination close to 1.0 indicates that the second-order polynomial accurately explains most of the variability in the response as a function of the studied parameters (pH, contact time, temperature, and initial concentration). Using the ANOVA test to evaluate the accuracy and validity of the model, Table 3 (Appendix) shows the results. The p-value determines the statistical significance of the relationship between the response and the parameters in the model, and the interaction effects can be considered significant when $p < 0.05$. A lower p-value represents the rejection of insignificant values.

3.3 Response surface methodology (RSM) analysis vs factor influence

To avoid extreme experimental conditions, the BBD focuses on the mid-points and borders of the experimental domain. These properties can make it adapted to develop quadratic models to accurately predict optimal conditions and examine the complicated interactions between the independent variables. To optimize SMX and TMP removal, BBD identifies how factors interact to influence the overall efficient removal. The results of the adsorption removal of TMP and SMX on Amp and AMb are shown in Table 3 (Appendix) and Table 4

(Appendix). The data was generated, and it was then analyzed and interpreted using NEMROD-W. The actual values were similar to the predicted values, as seen in Table 3 (Appendix) and Table 4 (Appendix). The experimental conditions of the design, the results obtained are the amount of R% measured (exp), and the predicted result R% (Calcul). BBD yields 27 runs (24 factorial + 3 center). Fit a second-order polynomial. The concentration and contact time are significant (p-value < 0.05) and strongly influence the response. While the effects of the following factors are not significant, their p-values > 0.05, and do not influence the response: temperature factors and the effect of T interactions *Contact time, temperature *pH. These factors are removed from the model equation.

Y1=72.000+5.592X1−11.725X2−22.467X3+0.150X4−13.925X12−2.950X22−19.812X32−14.687X42−4.375X1X2+0.225X1X3−0.825X2X3+0.725X1X4−8.975X2X4−0.200X3X4

With: X1X_1X1 is the temperature; X2X_2X2 is the TMP concentration; X3X_3X3 is the pH; X4X_4X4 is the contact time.

The model-corrected equation is written as follows:

$$Y1=72.000+5.592X1-11.725X2-22.467X3-13.925X1^2-19.812X3^2-14.687X4^2-8.975X2X4$$

Individual terms such as concentration and pH are the most influential coefficients in both models. However, their amplitudes may vary, indicating that one of the two antibiotics is more sensitive to one of these parameters than the other.

The analysis of the polynomial coefficients revealed that pH (X3) is the post-dominant and highly significant effect (p<0.001) for both adsorption antibiotics by the purified clay (AMb) when its linear and quadratic forms, confirming the sensitivity of the process to medium acidity. Table 5 (Appendix). Additionally, the increasing of pH markedly reduced removal efficiency due to electrostatic repulsion between negatively charged SMX molecules and the clay surface. The antibiotic concentration (X_2) also showed a significant negative effect ($p < 0.01$), indicating active-site saturation at higher initial loads. Meanwhile, quadratic terms for contact time (X_4^2) and temperature (X_1^2) displayed notable curvature, suggesting that adsorption improves up to optimal mid-level conditions before plateauing. Among the interaction terms, only concentration–time (X_2X_4) was significant ($p < 0.05$), implying that prolonged contact does not compensate for site saturation at high concentrations. Overall, the model demonstrates that optimal SMX removal occurs at moderate temperature and concentration, near-neutral pH, and intermediate contact time. This is explained by the electrostatic interaction between the surface charge of the adsorbent and the ionic charge of the molecules. Hence, at a low pH value, the surface of the clay could be more positively charged, which would promote stronger interactions with negatively ionized forms of antibiotics. The RSM Surface plots show that modified clay (AMp) offers a higher adsorption capacity (93.7%) than raw natural clay (80.7%), Figure 5 (Appendix), demonstrating the effectiveness of the modification to optimize antibiotics adsorption under optimal conditions. In order to identify the mechanism of the adsorption process, the adsorption isotherms were evaluated and analyzed. Different models of isotherms are available in the literature.

3.4 Adsorption isotherm

Kinetic studies of the adsorption process are needed to identify the phenomenon where surfactant molecules migrate from the bulk phase to the solid–liquid interface. Hence, the adsorption behavior in the porous system, as smectite, is a complex phenomenon.

3.4.1 Influence of contact time

The adsorption kinetics of sulfamethoxazole and trimethoprim on the two adsorbents are presented in Figure 6 (Appendix), the elimination of pharmaceuticals at different contact times, studied at a clay concentration of 25 $mg.L^{-1}$. The curves show that the kinetics of adsorption is very fast during the first ten minutes, due to the presence of vacant and abundant active sites on the adsorbent, following the molecular diffusion of ions towards the adsorption sites, then they tend towards a saturation plateau, where all the sites are occupied until reaching an equilibrium time of a maximum of 110 min which become saturated over time upon reaching equilibrium. The comparison of the studied materials allows us to conclude that the amount of SMX and that of TMP adsorbed on purified clay (250$mg.g^{-1}$) and (190$mg.g^{-1}$) are greater compared to that of the raw clay.

3.4.2 Adsorption isotherms and their modeling

The experimental results are modeled to better interpret the adsorption mechanisms of compounds such as sulfamethoxazole (SMX) and trimethoprim (TMP) by clay. The models used are those with two parameters (Langmuir and Freundlish) Table 6 (Appendix).

The results showed that the pseudo-first order equation does not give values in agreement with the experimental values for SMX and TMP because of their low linear regression values (R2), quite far from

1. Moreover, the calculated adsorption capacities were much lower than the experimental values. The pseudo-second order kinetic model provided the best fit, with R2 values of 0.99 and 0.98, which strongly confirms that the adsorption reflects a chemisorption behavior where the interaction between the surface and the availability of active sites on the clay (solid-liquid interface) is more predominant than the diffusion-controlled adsorption. Dual-site Langmuir model, usually used for multilayer adsorption systems, Figure 7 (Appendix) and Freundlich isotherm is an empirical model that can be used for multilayer adsorption on heterogeneous active sites, Figure 8 (Appendix). Regarding the treatment of isotherms, the results show that the adsorption follows both the 1800s and Freundlich models, with R2 correlation coefficients greater than 0.98 and 0.99, and values of the coefficient nf within the interval [0.1 - 0.5] This model assumes that the adsorption heat distribution and affinities towards the heterogeneous adsorbent surface are nonuniform. In addition, the results improve the role of the clay minerals in the expansion, which could do interaction on the internal and external surface, allowing the catching of molecules ‘antibiotics into smectite platelets

3.4.3 Effect of temperature and thermodynamic analysis

The efficiency of the adsorption process is studied by several interdependent factors. For the removal of sulfamethoxazole and trimethoprim using natural clay, a methodical approach is required to identify and optimize these critical parameters. Smectites have a permanent negative charge related to the isomorphous substitution in the structure. This charge allows cation exchange and the attraction of cationic or neutral species. The BBD model adequately explains the interaction of the temperature and other adsorption parameters, and BBD provides the framework to study these variables systematically. The results for both molecules indicated that the adsorption on smectite adsorbent decreases when the temperature increases. The temperature is a critical factor and important factor because it controls the behaviour of the adsorption process, and leads to affecting the adsorbate-adsorbent interaction in their system, which is strongly reliant on thermodynamic parameter values. The Van't Hoff plot (ln Ka vs1/T) is used to calculate the values of ΔG, ΔH, and ΔS. Adsorption of SMX and TMP on purified clay AMB have studied at temperatures ranging from 313 to 333. The outcomes are presented in Table 3. Under the experimental conditions, the SMX and TMP with negative ΔGº showed a favourable and spontaneous behaviour.

Table 3: Thermodynamic parameters of SMX and TMP adsorption on AMp. Source: created by authors.

	T(K)	ΔHº ($kJ.mol^{-1}$)	ΔGº ($kJ.mol^{-1}$)	ΔSº ($KJ.mol^{-1}K^{-1}$)
SMX	**313** **323** **333**	**-49.3**	**-50.52** **-50.56** **-50.60**	**3.9**
TMP	**313** **323** **333**	**-49.2**	**-50.48** **-50.53** **-50.56**	**4.1**

$$\ln\left(\frac{q}{c_e}\right) = \frac{\Delta S^0}{R} - \frac{\Delta H^0}{RT} \quad (3)$$

$$\Delta G^o = \Delta H^o - \Delta S^o \quad (4)$$

Where T is the temperature in Kelvin, R is the gas constant ($8.314\ J^{-1}.mol^{-1}.K^{-1}$). Determine the Slop and intercept pf the plots between ln (qe/Ce) vs 1/T to engage the ΔGo, ΔSo, and ΔHo. The Combine of the Box–Behnken statistical modeling and thermodynamic analysis provides a comprehensive understanding of SMX and TMP adsorption through natural AMb clay. The BBD model identified that the efficiency of the removal of TMP increases at lower temperatures, while the thermodynamic results revealed a spontaneous process and exothermic for both TMP and SMX (ΔH° < 0). This is explained by the favor strong adsorbate/adsorbent interactions at low temperature, with the interparticle diffusion and surface diffusion mechanisms. The positive entropy (ΔSº =3.9 $KJ.mol^{-1}K^{-1}$ for the SMX and ΔSº =4.1$KJ.mol^{-1}K^{-1}$ for TMP) indicates that the physicochemical adsorption mechanism involves hydrogen bonding, electrostatic attraction, and π–π interactions. This combined approach predicted a vigorous optimization of operating conditions for efficient antibiotic removal using natural clays in water treatment applications. Additionally, the temperature is necessary to allow for the diffusion of antibiotic molecules into the clay pores and interaction with active sites, [29], [30]. The adsorption mechanisms generally involve the electrostatic interactions with surface hydroxyl groups and ion exchange reactions at constantly charged sites. Within the pH range of 5 and 6, the SMX exists in its negative charge species due to the deprotonation of the sulfonamide group above the pKa =5.7, which could make the electrostatic attraction and ion exchange favorable with positively charged exchange sites on smectite surfaces. For the TMP with pKa= 7, it is partially protonated under these conditions, and it may easily enhance its affinity for the negative charge of the clay surfaces through cation exchange and electrostatic attraction, [31]. The Tow adsorbents, raw clay (AMb) and purified smectite (AMb)shows a good adsorption capacity for both SMX and TMP, attributed to the removal of impurities and increasing the exposure of active sites.

3.5 Analyzing the effectiveness of clay compared to other adsorbents

Various treatment techniques have been studied to remove sulfamethoxazole and trimethoprim from wastewater and aquatic environments, including adsorption on porous materials, using different adsorbents, including other types of clay, resins, and nanoparticles. As part of this study, it is important to compare the efficiency and capacity of Tunisian natural clay with other adsorbents. Table 7 (Appendix) present the works that use adsorbents are considered environmentally friendly. These data show that the natural clay based on smectite and alumina used in this study is a very competitive adsorbent, with an adsorption efficiency of SMX exceeding 80%, and 90% for TMP. Natural clays have many advantages as adsorbents, due to the fact that its higher surface area, which offers numerous active sites for pollutant binding, and a high cation exchange capacity (CEC) that enables effective adsorption of charged species [20], [28], [38]. Their layered structure promotes intercalation and surface interactions with organic molecules. Additionally, clays are cost-effective and widely available, making them suitable for large-scale and sustainable environmental applications. Furthermore, their modifiability through chemical or physical treatments allows enhancement of adsorption performance, selectivity, and capacity.

4 Conclusion

The persistent presence of pharmaceuticals Sulfamethoxazole (SMX) and Trimethoprim (TMP) in aquatic environments poses a crucial ecological and health risks mainly contributing to antibiotic resistance. Their widespread use means they are frequently detected in wastewater and natural aquatic environments. This study investigates the use of clays in the treatment of water containing emerging pollutants, particularly pharmaceutical products used in the fish farming sector. The purification of AM clay, based on the methods described in the literature, was characterized by appropriate physicochemical analysis methods to define its structural properties and chemical composition. The parameters of this process, in batch mode, have been modeled and optimized using a Box-Behnken (BBD) response surface-type experimental design, where adsorption removal on AAM is almost complete with a yield exceeding 80% for SMX and 90% for TMP. Based on the statistical model, optimal conditions that maximize SMX and TMP removal are predicted. These predicted optimal conditions are then experimentally validated to confirm the model's accuracy. Contour plots and three-dimensional response surface plots have visualized the effects of multiple factors and their interactions on the adsorption efficiency. The pH control (5-6) and initial concentration (55 mg. L-1) are highly influential factors in optimizing the adsorption of SMX and TMP, often having the most significant impact on removal efficiency. While initial contact time (80) has a moderate but important effect, ensuring equilibrium is reached. Temperature, despite being influential, may have a slightly smaller direct impact than other parameters in typical ambient conditions for batch adsorption studies.

References:

[1] A. Pal, K. Y.-H. Gin, A. Y.-C. Lin, M. Reinhard, Impacts of emerging organic contaminants on freshwater resources: Review of recent occurrences, sources, fate and effects, *Science of the Total Environment*, Vol. 408, No. 24, 2010, pp. 6062–6069. https://doi.org/10.1016/j.scitotenv.2010.09.026

[2] T. Cherian, C. Ragavendran, S. Vijayan, S. Kurien, W. J. G. M. Peijnenburg, A review on the fate, human health and environmental impacts, as well as regulation of antibiotics used in aquaculture, *Environmental Advances*, Vol. 13, 2023, pp. 100411. https://doi.org/10.1016/j.envadv.2023.100411

[3] Seafood Watch, Understanding the use and impact of antibiotics in aquaculture, Monterey Bay Aquarium, *Seafood Sustainability Series*, Vol. 1, 2023. https://www.seafoodwatch.org/ [Access Date: 01/01/2026]

[4] A. El Badawy, D. Hamza, Z. Ahmed, M. A. Sabry, Seasonal and environmental drivers of antibiotic resistance and virulence in Escherichia coli from aquaculture and their public health implications, *Scientific Reports*, Vol. 15, 2025, pp. 16100. https://doi.org/10.1038/s41598-025-98498-8

[5] T.-Y. Wang, M. Cheng, X. Wang, H.-R. Zhu, A. Huang, N. Zhang, X.-D. Hao, L.-T. Hao, C. Shi, Characteristics, impacts and high-efficiency treatment technologies for antibiotic residues in aquaculture wastewater: A review, *SSRN*

Electronic Journal, 2024. https://doi.org/10.2139/ssrn.5046669

[6] Y. Aissaoui, G. Jiménez-Skrzypek, J. González-Sálamo, M. Trabelsi-Ayadi, I. Ghorbel-Abid, J. Hernández-Borges, Determination of Multiclass Antibiotics in Fish Muscle Using a QuEChERS-UHPLC-MS/MS Method, *Foods*, Vol. 13, No. 7, 2024, p. 1081. https://doi.org/10.3390/foods13071081

[7] U. Salma, A. Hossain, M. Shafiujjaman, Y. Nishimura, M. Tokomura, R. Tanoue, T. Kunisue, K. Watanabe, M. Raknuzzaman, T. Amagai, M. Makino, Occurrence, risks, and mitigation of antibiotic pollution in Bangladeshi aquaculture systems, *Environmental Chemistry & Ecotoxicology,* Vol. 7, 2025, pp. 351-363. https://doi.org/10.1016/j.enceco.2025.01.007

[8] D. Schar, E. Y. Klein, R. Laxminarayan, M. Gilbert, T. P. Van Boeckel, Global trends in antimicrobial use in aquaculture, *Scientific Reports*, Vol. 10, 2020, pp. 21878. https://doi.org/10.1038/s41598-020-78849-3

[9] M. Pepi, S. Focardi, Antibiotic-resistant bacteria in aquaculture and climate change: A challenge for health in the Mediterranean area, *International Journal of Environmental Research and Public Health*, Vol. 18, No. 11, 2021, pp. 5723. https://doi.org/10.3390/ijerph18115723

[10] B. Habibi, I. Ghorbel-Abid, R. Lahsini, D. Chehimi Ben Hassen, M. Trabelsi-Ayadi, Development and validation of a rapid HPLC method for multiresidue determination of erythromycin, clarithromycin, and azithromycin in aquaculture fish muscles, *Acta Chromatographica,* Vol. 31, No. 2, 2019, pp. 109–112. https://doi.org/10.1556/1326.2017.00376

[11] F. Fenni, A. Sunyer-Caldú, H. Ben Mansour, M. S. Diaz-Cruz, Occurrence and risks of pharmaceuticals in Mahdia's coastline (Tunisia): Distribution, antibiotic resistance, and ecotoxicological impact, *Environmental Science and Pollution Research*, Vol. 32, 2025, pp. 18419–18433. https://doi.org/10.1007/s11356-025-36743-3

[12] F. C. Cabello, H. P. Godfrey, A. H. Buschmann, H. J. Dölz, Aquaculture as yet another environmental gateway to the development and globalisation of antimicrobial resistance, *The Lancet Infectious Diseases*, Vol. 16, No. 7, 2016, pp. 127–133. https://doi.org/10.1016/S1473-3099(16)00100-6

[13] D. Coêlho de Sá Júnior, R. B. Vieira, G. U. de Souza Cruz, G. de A. L. F. Furtado, B. P. Oliveira, F. M. D. Bastos, I. F. Batista, V. C. O. Silva, C. A. de O. A. Neto, I. G. Santos, L. M. L. S. L. Costa, A. L. de P. M. Zanina, K. N. Marinho, L. G. Pereira, L. T. Tavares, M. E. S. Albuquerque, S. L. G. P. Cardoso, The impact of climate change on infectious diseases and antibiotic resistance, *International Journal of Advanced Engineering Research and Science*, Vol. 11, No. 2, 2024, pp. 14–18. https://doi.org/10.22161/ijaers.112.3

[14] E. S. Okeke, K. I. Chukwudozie, R. Nyaruaba, R. E. Ita, A. Oladipo, O. Ejeromedoghene, E. O. Atakpa, C. V. Agu, C. O. Okoye, Antibiotic resistance in aquaculture and aquatic organisms: A review of current nanotechnology applications for sustainable management, *Environmental Science and Pollution Research*, Vol. 29, 2022, pp. 69241–69274. https://doi.org/10.1007/s11356-022-22319-y

[15] M. von Ahnen, K. Tang, I. van de Ven, A. C. Hambly, H. R. Andersen, N. Lorenzen, P. B. Pedersen, Removal of residual antibiotics from aquaculture effluents by denitrifying woodchip bioreactors, *Aquaculture*, Vol. 608, 2025, pp. 742761. https://doi.org/10.1016/j.aquaculture.2025.742761

[16] Y. L. Shang, M. Huang, L. Zhao, P. He, Y. Liu, H. Pan, S. Cao, X. Liu, Adsorption performance and mechanisms of tetracycline on montmorillonite, *ACS Omega*, Vol. 9, No. 1, 2024, pp. 692–699. https://doi.org/10.1021/acsomega.3c06478

[17] L. Mahouachi, T. Rastogi, W. Palm, I. Ghorbel-Abid, D. Chehimi Ben Hassen, K. Kümmerer, Natural clay as a sorbent to remove pharmaceutical micropollutants from wastewater, *Chemosphere*, Vol. 258, 2020, pp. 127213. https://doi.org/10.1016/j.chemosphere.2020.127213

[18] H. Abd-ElFattah, R. Kamel, A. Maged, S. Kharbish, Harnessing clays and clay composites for efficient removal of pharmaceutical contaminants from water: A review, *Frontiers in Scientific Research and Technology*, Vol. 10, No. 1, 2025, pp. 85–100. https://doi.org/10.21608/fsrt.2025.344419.1143

[19] G. G. Hacıosmanoğlu, C. Mejías, J. Martín, J. L. Santos, I. Aparicio, E. Alonso, Antibiotic adsorption by natural and modified clay minerals as designer adsorbents for wastewater

treatment: A comprehensive review, *Journal of Environmental Management*, Vol. 317, 2022, pp. 115397. https://doi.org/10.1016/j.jenvman.2022.115397

[20] G. E. P. Box, D. W. Behnken, Some new three-level designs for the study of quantitative variables, *Technometrics,* Vol. 2, 1960, pp. 455–475. https://doi.org/10.1080/00401706.1960.10489912

[21] I. Maldonado, A. P. Vega Quispe, M. Gutiérrez, Optimization of the elimination of antibiotics by Lemna gibba and Azolla filiculoides using response surface methodology, *Frontiers in Environmental Science*, Vol. 10, 2022, pp. 940971. https://doi.org/10.3389/fenvs.2022.940971

[22] A. Kazemi, E. Ebrahimpour, M. Esmaeilbeigi, F. Gheitasi, F. Einollahipeer, M. Mohammadrezai, Optimizing oxytetracycline removal from aqueous solutions using activated carbon from barley lignocellulosic wastes: Isotherms and thermodynamic studies, Scientific Reports, Vol. 14, 2024, No. 21629. https://doi.org/10.1038/s41598-024-73142-z

[23] M. A. Zamiri, J. Wang, C. H. Niu, Competitive adsorption and molecular interaction study of sulfamethoxazole and trimethoprim on biomass-based activated carbon, *Chemosphere,* Vol. 385, 2025, No. 144591. https://doi.org/10.1016/j.chemosphere.2025.144591

[24] S. Barakan, V. Aghazadeh, A. Samiee Beyragh, S. Mohammadi, Thermodynamic, kinetic and equilibrium isotherm studies of As(V) adsorption by Fe(III)-impregnated bentonite, *Environment, Development and Sustainability*, Vol. 22, 2020, pp. 5273–5295. https://doi.org/10.1007/s10668-019-00424-2

[25] Ahmad Khan, Mohammad Saleem Akhtar, Saba Akbar, Khalid Saifullah Khan, Mazhar Iqbal, Ana Barrientos‑Velazquez, Youjun Deng, Effects of metal-polycation pillaring and exchangeable cations on aflatoxin adsorption by smectite, *Clays and Clay Minerals*, Vol. 70, No. 2, 2022, pp. 155–164. https://doi.org/10.1007/s42860-021-00159-0

[26] C. J. Wang, Z. Li, W. T. Jiang, J. S. Jean, C. C. Liu, Cation exchange interaction between antibiotic ciprofloxacin and montmorillonite, Journal of Hazardous Materials, Vol. 183, 2010, pp. 309–314. https://doi.org/10.1016/j.jhazmat.2010.07.025

[27] J. D. Russell, A. R. Fraser, Spectroscopic and chemical determinative methods, in Clay Mineralogy, *Springe*r, 1994, pp. 11–67. https://doi.org/10.1007/978-94-011-0727-3_2

[28] (text in Chinese) Y. J. Zhang, W. Y. Dong, H. Wang, G. K. Yan, Y. Chang, H. Wang, Y. Ling, Adsorption effect and mechanism of sulfamethoxazole and trimethoprim on corncob, *Journal of Environmental Engineering Technology,* Vol. 13, No. 3, 2023, pp. 1108–1117. https://doi.org/10.12153/j.issn.1674-991X.20220375

[29] C. Mejías, J. L. Santos, J. Martín, I. Aparicio, E. Alonso, Thermodynamic and kinetic investigation of the adsorption and desorption of trimethoprim and its main metabolites in Mediterranean crop soils, *Molecules*, Vol. 28, No. 1, 2023, Article No. 437. https://doi.org/10.3390/molecules28010437

[30] S. Jodeh, A. Jaber, G. Hanbali, Y. Massad, Z. S. Safi, S. Radi, V. Mehmeti, A. Berisha, S. Tighadouini, O. Dagdag, Experimental and theoretical study for removal of trimethoprim from wastewater using organically modified silica with pyrazole-3-carbaldehyde bridged to copper ions, *BMC Chemistry*, Vol. 16, 2022, p. 17. https://doi.org/10.1186/s13065-022-00814-0

[31] T. De Oliveira, E. Fernandez, L. Fougère, E. Destandau, M. Boussafir, M. Sohmiya, Y. Sugahara, R. Guégan, Competitive association of antibiotics with a clay mineral and organoclay derivatives as a control of their lifetimes in the environment, *ACS Omega,* Vol. 3, No. 11, 2018, pp. 15332–15342. https://doi.org/10.1021/acsomega.8b02049

[32] S. Chianese, A. Fenti, J. Blotevogel, D. Musmarra, P. Iovino, Trimethoprim removal from wastewater: Adsorption and electrooxidation comparative case study, *Case Studies in Chemical and Environmental Engineering*, Vol. 8, 2023, p. 100433. https://doi.org/10.1016/j.cscee.2023.100433

[33] R. Li, W. Sun, L. Xia, Z. U., X. Sun, Z. Wang, Y. Wang, X. Deng, Adsorption of Toxic Tetracycline, Thiamphenicol and Sulfamethoxazole by a Granular Activated Carbon (GAC) under Different Conditions, *Molecules,* Vol. 27, No. 22, 2022, p. 7980. https://doi.org/10.3390/molecules27227980

[34] R. Lavecchia, A. Zuorro, O. Baaloudj, M. Brienza, Trimethoprim removal from aqueous solutions via volcanic ash-soil adsorption: process modeling and optimization, *Water*, Vol. 16, No. 15, 2024, p. 2209. https://doi.org/10.3390/w16152209

[35] J. Berges, S. Moles, M. P. Ormad, R. Mosteo, J. Gómez, Antibiotics removal from aquatic environments: Adsorption of enrofloxacin, trimethoprim, sulfadiazine, and amoxicillin on vegetal powdered activated carbon, Environmental Science and Pollution Research, Vol. 28, 2021, pp. 8442–8452. https://doi.org/10.1007/s11356-020-10972-0

[36] A. Mirzaei, L. Yerushalmi, Z. Chen, F. Haghighat, Photocatalytic degradation of sulfamethoxazole by hierarchical magnetic ZnO@g-C_3N_4: RSM optimization, kinetic study, reaction pathway and toxicity evaluation, *Journal of Hazardous Materials*, Vol. 359, 2018, pp. 516–526. https://doi.org/10.1016/j.jhazmat.2018.07.077

[37] Y. Ou, X. Zhang, H. Li, L. Wang, Magnetically separable Fe-MIL-88B_NH_2 carbonaceous nanocomposites for efficient removal of sulfamethoxazole from aqueous solutions, *Journal of Colloid and Interface Science*, Vol. 570, 2020, pp. 163–172. https://doi.org/10.1016/j.jcis.2020.02.116

[38] Y. He, C. Liu, X-Yu. Tang, Q-S. Xian, J-Q. Zhang, Z. Guan, Biochar impacts on sorption-desorption of oxytetracycline and florfenicol in an alkaline farmland soil as affected by field ageing, *Science of The Total Environment*, Vol. 671, 2019, pp. 928-936. https://doi.org/10.1016/j.scitotenv.2019.03.414

Contribution of Individual Authors to the Creation of a Scientific Article (Ghostwriting Policy)

All authors equally contributed to the development of the article.

Sources of Funding for the Research Presented in the Scientific Article or for the Scientific Article Itself

No funding was received for conducting this study.

Conflict of Interest

The authors declare that they have no conflicts of interest relevant to the content of this article.

APPENDIX

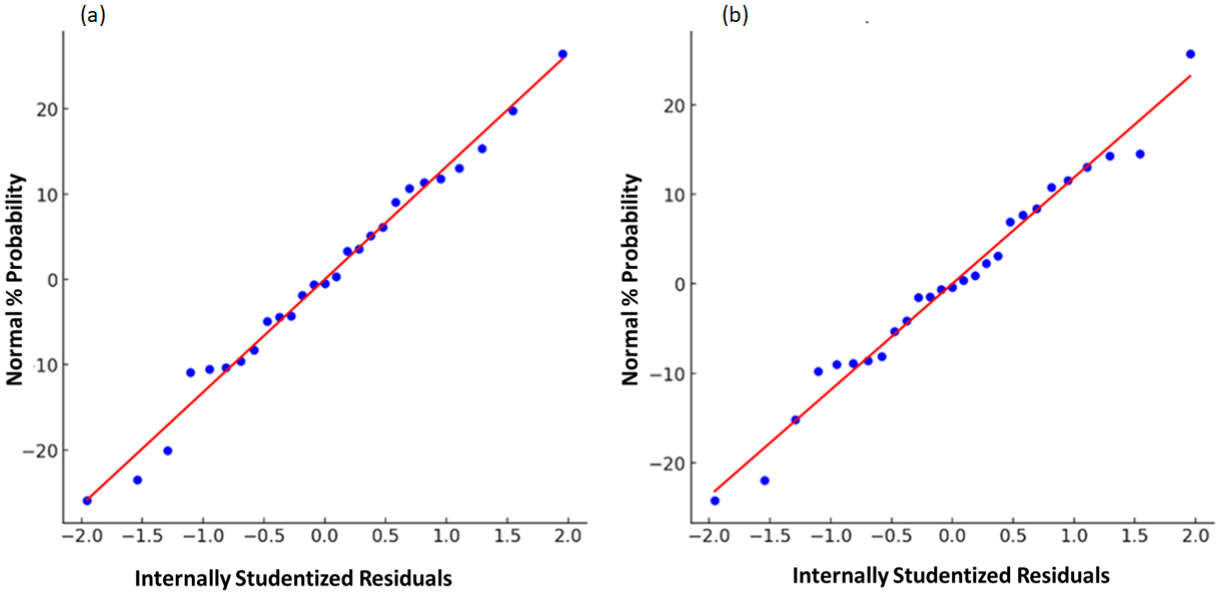

Fig. 1: Normal plot of residuals for (a) TMP and (b) SMX. Source: created by authors.

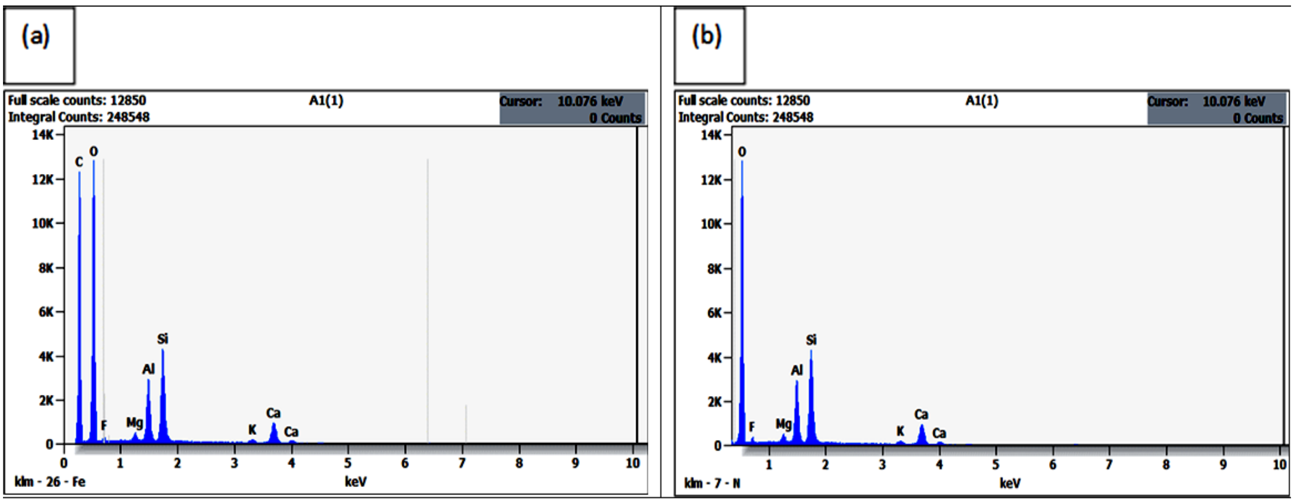

Fig. 2: EDS Spectrums of raw natural c(a) and purified clay (b)
Source: created by authors.

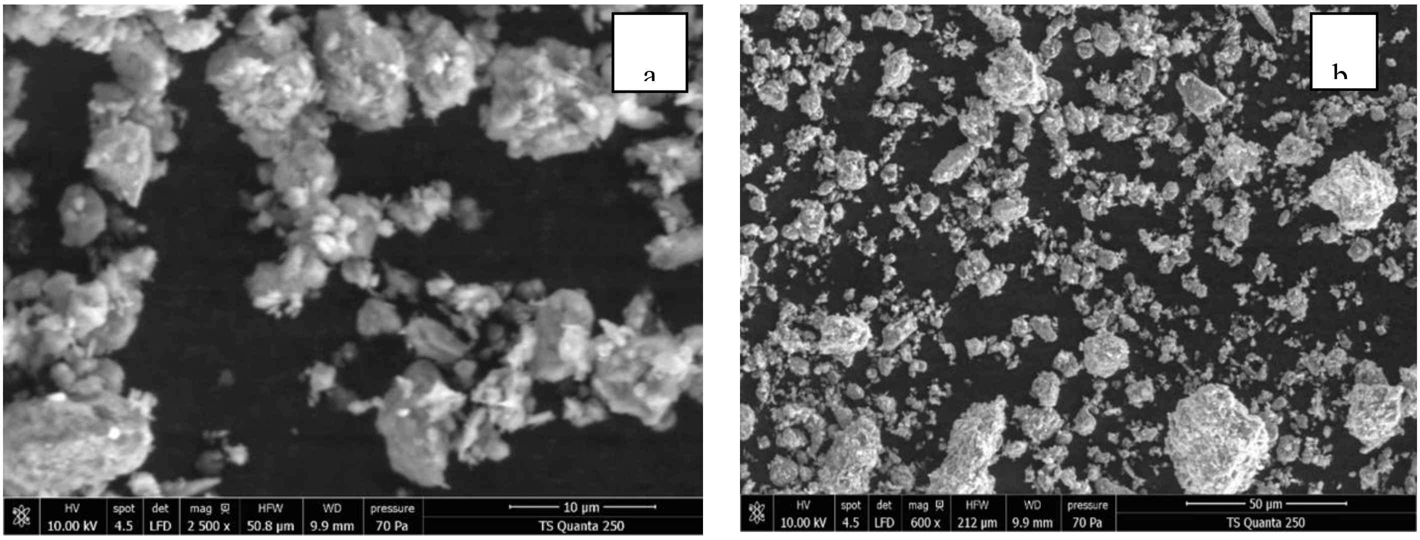

Fig. 3: Scanning electron microscope micrographs of the tested clay adsorbents: raw clay (a) and purified clay (b).
Source: created by authors

Fig. 4: XRD patterns (b) of the tested clay-based adsorbents. Source: created by authors.

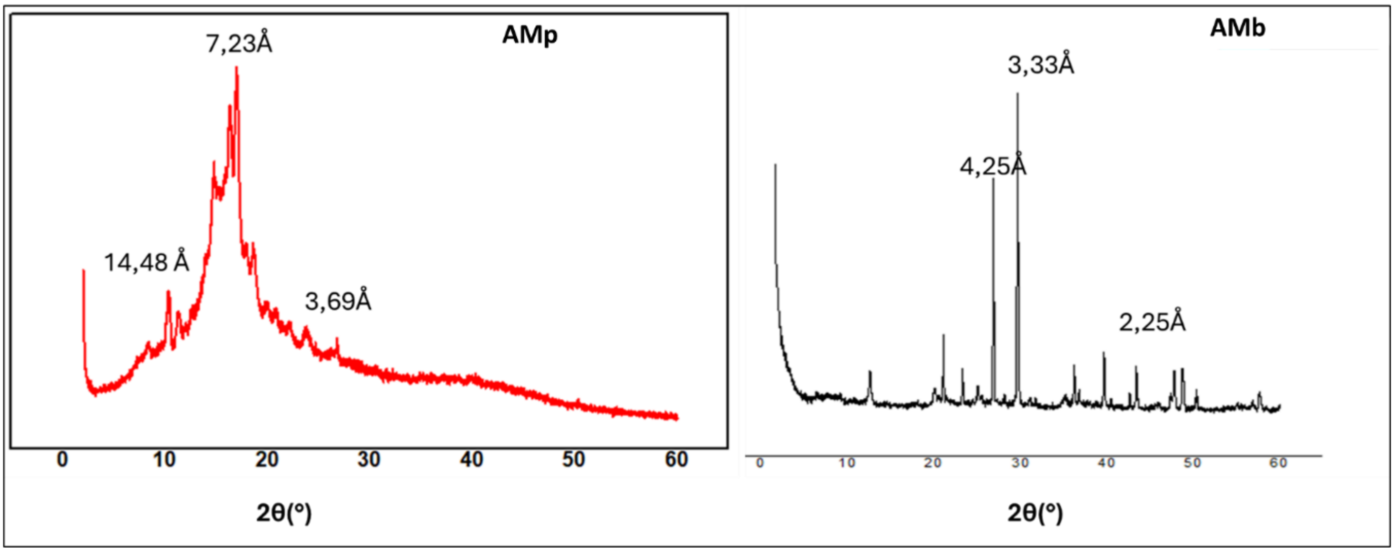

Yousra Aissaoui, Malika Trabelsi-Ayadi,
Ibtissem Ghorbel-Abid

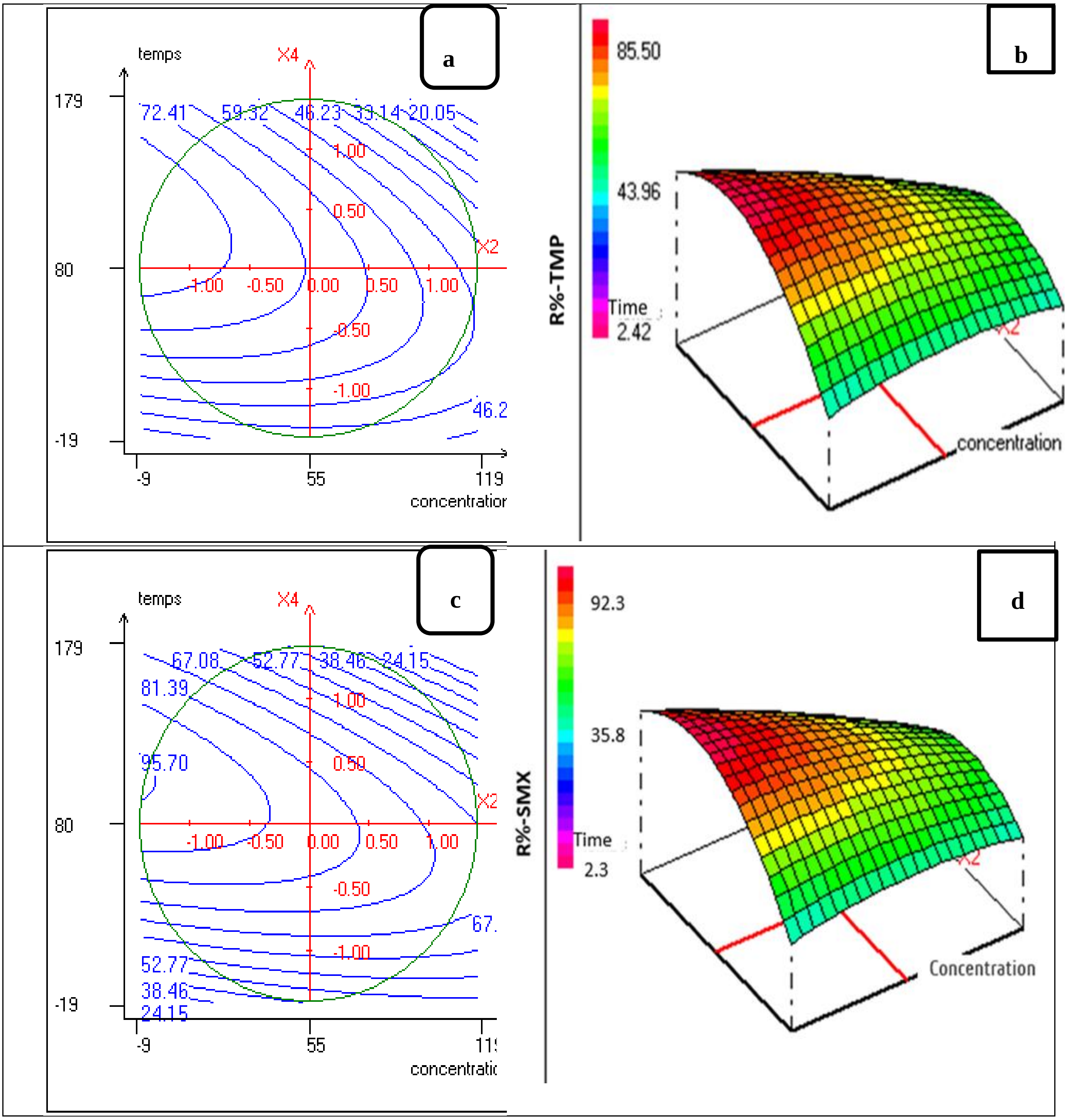

Fig. 5: Curves of isoresponses of the TMP and SMX adsorption.
Source: created by authors
a: Curve of the efficiency of the removal of TMP adsorption by AMp
b: Variation in the elimination rate of TMP adsorption by AMb
c: Curve of the efficiency of the removal of SMX adsorption by Amp
d: Variation of the elimination rate of SMX adsorption by AMb

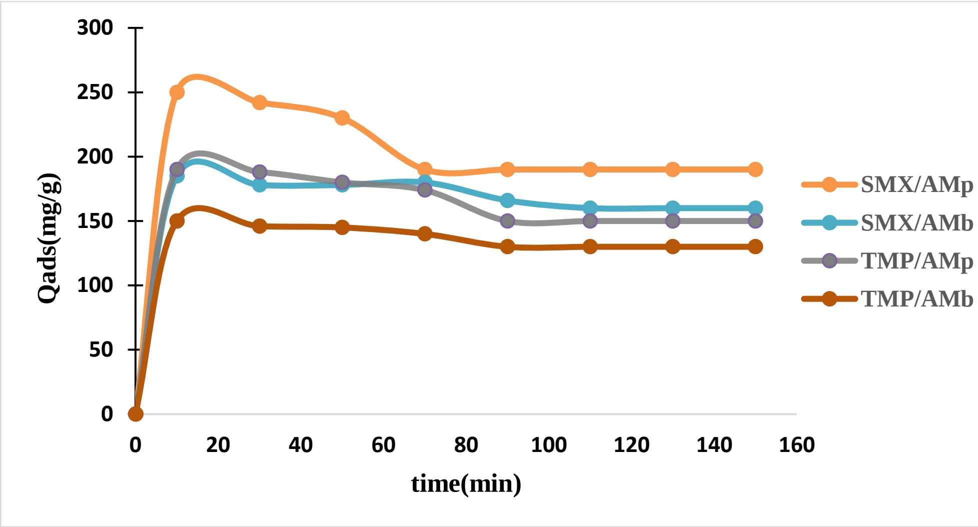

Fig. 6: Influence of the contact time on the adsorption of SMX and TMP on AMp and AMb (T =25°C; C_0 =50 mg. L^{-1}; $C_{adsorbant}$=25 mg. L^{-1}).
Source: created by authors.

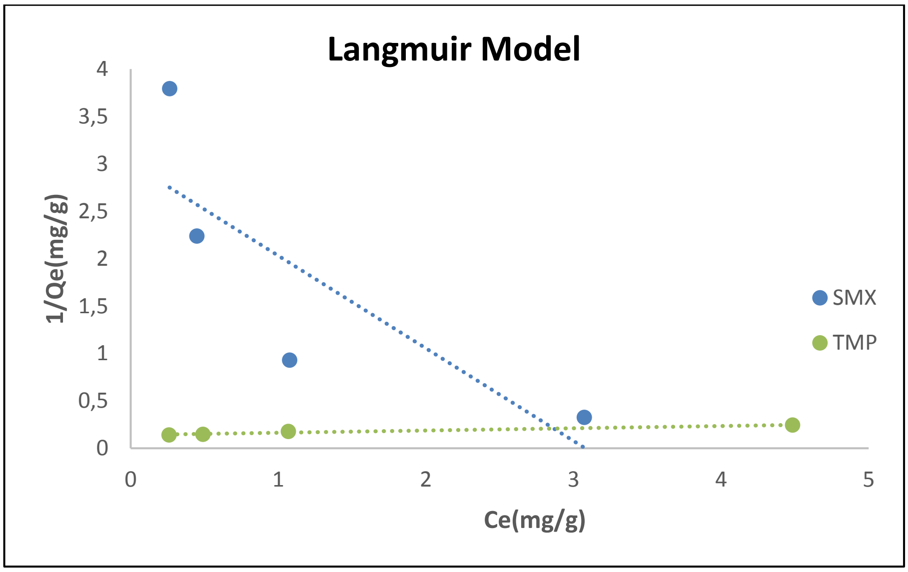

Fig. 7: Isotherms of the Langmuir model.
Source: created by authors.

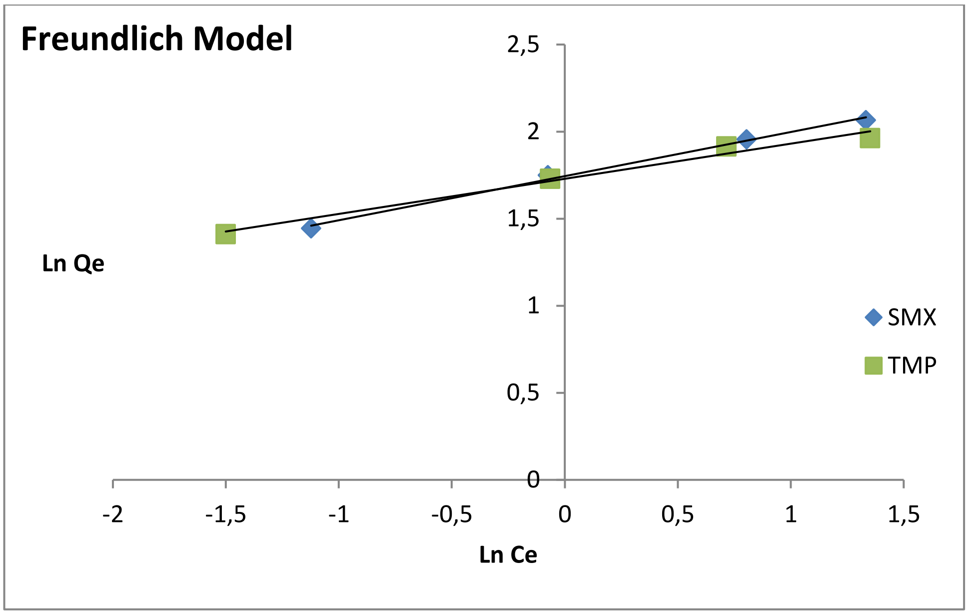

Fig. 8: isotherms linearized by the Winchester model -
Adsorption of SMX and TMP by AAMp. (C_0 = 50 mg. L^{-1}, T = 25 °C and pH= 6).
Source: created by authors.

Table 1: Physicochemical properties of the target antibiotics

Compound	Molecular structure	Log K_{ow}	pKa	Water solubility (mg. L^{-1})
Sulfamethoxazole	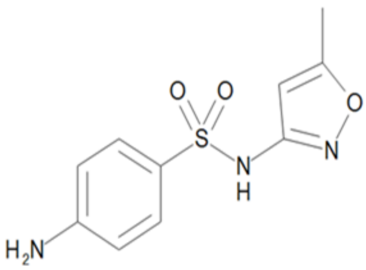	0.89	1.60-5.70	77
Trimethoprim	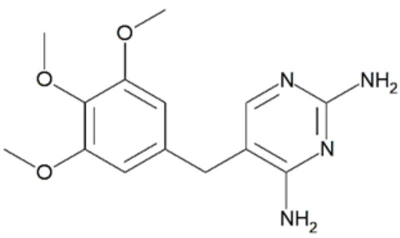	0.91	1.32-7.45	400

Source: created by authors

Table 2: Chemical composition of the tested clay adsorbents

Purified Clay		
Element	***Weight %***	***Atom %***
O	54.90	69.76
F	1.58	1.69
Mg	1.01	0.84
Al	9.30	7.00
Si	17.67	12.79
K	1.76	0.91
Ca	13.79	7.00
Total	100.00	100.00
Raw Caly (AMb)		
Element	***Weight %***	***Atom %***
C	23.62	33.59
O	45.09	48.13
F	3.07	2.76
Mg	0.65	0.46
Al	6.04	3.82
Si	11.36	6.90
K	1.15	0.50
Ca	9.02	3.85
Total	100.00	100.00

Source: created by authors.

Table 3: The 3-factor BBD matrix, experimental and predicted values for TMP removal by AMb and AMp.

N	**Temperature**	**Concentration**	**pH**	**Contact time**	**Y1 exp *R*(%) Adsorption by (AMb)**	**Y 1 Calcul (R%)**	**Y2 exp R (%) Adsorption by (AMp)**	**Y 2 Calcul (R%)**
1	40	10	6.5	80.0	64.6	56.883	76.7	75.146
2	80	10	6.5	80.0	85.5	76.817	95.7	86.763
3	40	100	6.5	80.0	42.3	42.183	54.8	60.779
4	80	100	6.5	80.0	54.7	44.617	75.3	63.896
5	40	55	4.0	80.0	53.4	55.363	85.7	80.929
6	80	55	4.0	80.0	61.0	66.096	75.8	78.146
7	40	55	9.0	80.0	15.8	9.979	19.3	15.396
8	80	55	9.0	80.0	24.3	21.613	29.7	32.913
9	40	55	6.5	10.0	32.9	38.371	45.7	50.858
10	80	55	6.5	10.0	44.8	48.104	45.3	50.725
11	40	55	6.5	150.0	31.0	37.221	35.7	44.792
12	80	55	6.5	150.0	45.8	49.854	50.3	59.658
13	60	10	4.0	80.0	73.8	82.604	89.3	97.408
14	60	100	4.0	80.0	65.3	60.804	77.5	78.592
15	60	10	9.0	80.0	25.3	39.321	28.4	41.825
16	60	100	9.0	80.0	13.5	14.221	17.0	23.408
17	60	10	6.5	10.0	59.7	56.963	60.5	56.863
18	60	100	6.5	10.0	48.5	51.463	55.8	61.646
19	60	10	6.5	150.0	78.9	75.213	89.1	81.696

20	60	100	6.5	150.0	31.8	33.813	37.6	39.679
21	60	55	4.0	10.0	65.4	59.617	68.9	65.596
22	60	55	9.0	10.0	18.3	15.083	22.8	13.313
23	60	55	4.0	150.0	65.9	60.317	73.6	70.129
24	60	55	9.0	150.0	18.0	14.983	21.3	11.646
25	60	55	6.5	80.0	72.0	72.000	85.6	85.600
26	60	55	6.5	80.0	72.0	72.000	85.6	85.600
27	60	55	6.5	80.0	72.0	72.000	85.6	85.600

Source: created by authors.

Table 4: The 3-factor BBD matrix, experimental and predicted values for SMX removal by AMb and AMP.

N	Temperature	Concentration	pH	Contact Time	Y1 exp *R*(%) Adsorption SMX by AMb	Y 1 Calcul (R%)	Y2 exp R (%) Adsorption SMX by (AMp)	Y2 Calcul (R%)
1	40	10	6.5	80.0	59.7	54.3	68.32	65.32
2	80	10	6.5	80.0	79.2	76.7	99.2	97.8
3	40	100	6.5	80.0	76.7	73.9	82.7	80.8
4	80	100	6.5	80.0	60.9	57.8	60.9	58.7
5	40	55	4.0	80.0	80.7	78.3	93.7	91.5
6	80	55	4.0	80.0	45.4	43.7	45.4	43.8
7	40	55	9.0	80.0	18.3	16.4	35.3	32.6
8	80	55	9.0	80.0	25.9	21.6	40.2	38.9
9	40	55	6.5	10.0	55.3	52.7	62.8	60.4
10	80	55	6.5	10.0	61.6	58.9	66.7	64.3
11	40	55	6.5	150.0	45.6	43.8	54.8	52.7
12	80	55	6.5	150.0	57.6	56.8	69.3	68.7
13	60	10	4.0	80.0	78.8	75.9	88.68	86.5
14	60	100	4.0	80.0	75.3	73.7	83.7	81.5
15	60	10	9.0	80.0	48.7	44.6	57.6	55.9
16	60	100	9.0	80.0	17.9	15.4	23.5	21.4
17	60	10	6.5	10.0	49.8	46.3	56.8	54.3
18	60	100	6.5	10.0	45.3	42.8	61.3	58.7
19	60	10	6.5	150.0	39.3	36.7	52.9	49.7
20	60	100	6.5	150.0	24.3	23.6	35.7	33.6
21	60	55	4.0	10.0	81.9	79.3	92.3	90.7
22	60	55	9.0	10.0	27.7	25.6	32.8	29.7
23	60	55	4.0	150.0	68.4	67.3	75.8	75.4
24	60	55	9.0	150.0	14.3	11.9	14.9	11.6
25	60	55	6.5	80.0	35.3	35.1	47.1	45.8
26	60	55	6.5	80.0	35.7	35.1	46.8	44.3
27	60	55	6.5	80.0	35.9	35.1	46.8	44.3

Source: created by authors.

Table 5: Regression coefficients obtained for the RSM-generated model.

Nom	Coefficient	Value	SD-Error	t-value	Signif. %
b0	85.600		5.552	15.42	***
b1	3.683	1.00	2.776	1.33	20.7%
b2	-9.308	1.00	2.776	-3.35	**
b3	-27.692	1.00	2.776	-9.98	***
b4	0.717	1.00	2.776	0.26	79.6%
b11	-11.208	1.25	4.164	-2.69	*
b22	-2.746	1.25	4.164	-0.66	52.8%
b33	-22.546	1.25	4.164	-5.41	***
b44	-22.883	1.25	4.164	-5.50	***
b12	-2.125	1.00	4.808	-0.44	66.9%
b13	5.075	1.00	4.808	1.06	31.3%
b23	0.100	1.00	4.808	0.02	98.1%
b14	3.750	1.00	4.808	0.78	45.6%
b24	-11.700	1.00	4.808	-2.43	*
b34	-1.550	1.00	4.808	-0.32	75.0%

Source: created by authors.

Table 6: Parameters of isotherms and their modeling. Source: created by authors.

Model	Parameter/Unity	SMX	TMP
Pseudo-first order kinetic model	qe ($mg.g^{-1}$) k^1 (min^{-1}) R^2	150 0,0205 0,2966	90 0,0357 0,6316
Pseudo Second Order Kinetic model	qe ($mg.g^{-1}$) k2 ($g.mg^{-1}.min^{-1}$) R2	150 0,060 0,9897	90 0,054 0.9993
experimental value	qe ($mg.g^{-1}$)	150	90
Langmuir	qm exp ($mg.g^{-1}$) KL R^2	0,332 0,9768 0,6679	7,136 0,0236 0,9693
Freundlich	nf Kf R^2	0,2018 5,645 0.9804	0,2533 5,725 0,9948

Table 7: Comparing the results found with those found in the literature. Source: created by authors.

Adsorbent	**Analyte**	**C_o (mg. L^{-1})**	**Amount of adsorbent**	**pH**	**Time (min)**	**Removal R%**	**Ref**
Activate carbon F400	TMP	10	50mg	7	30	70,6	[32]
Granular Activate carbon	SMX	25	4g	7	100	94,4	[33]
Soil with volcanic ashes	TMP	4,5	0,01-0,05	7,5	45,5	77,59	[34]
Activated charcoal in vegetable powder	TMP	15	100 mg	6	30	53	[35]
Hierarchical composite based on magnetic zinc oxideZnO@g-C3N4	SMX	30	0,65g	5,6	60	90,4	[36]
Nano-composites carbone Fe-MIL-88B_NH2	SMX	100	25mg	6	720	73,53	[37]
Natural clay @ Smectite-Alumine purified	SMX	55	100 mg	6,5	80	85,5	This study
Natural clay @Smectite-Alumine purified	TMP	55	100 mg	6	80	92,7	This study

.